



Atropisomeric small molecule Bcl-2 ligands: Determination of bioactive conformation

John Porter*, Andrew Payne, Ian Whitcombe, Ben de Candole, Daniel Ford, Rachel Garlish, Adam Hold, Brian Hutchinson, Graham Trevitt, James Turner, Chloe Edwards, Clare Watkins, Jeremy Davis, Colin Stubberfield

UCB Celltech, 216 Bath Road, Slough SL1 3WE, UK

ARTICLE INFO

Article history:

Received 3 December 2008

Revised 20 January 2009

Accepted 22 January 2009

Available online 27 January 2009

Keywords:

Bcl-2
Protein–protein interaction
Apoptosis
Atropisomerism

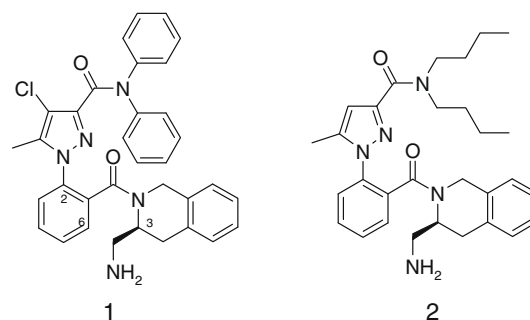
ABSTRACT

The separation of atropisomeric conformers of 1,2,3,4-tetrahydroisoquinoline amide Bcl-2 ligands allowed the identification of the bioactive conformer which was subsequently confirmed by X-ray crystallography.

© 2009 Elsevier Ltd. All rights reserved.

Regulation of cell death is of fundamental importance. Bcl-2 is a member of a family of anti- and pro-apoptotic proteins that function by binding to and sequestering other family members.¹ In healthy cells, Bcl-2 expression is tightly controlled, but it is overexpressed in a wide range of human haematopoietic and solid cancers where it serves to prevent apoptosis induced by protective cell-death mechanisms. This is manifested clinically as drug resistance when treating with traditional cytotoxics and can also delay apoptosis in response to radiation therapy.² The homologous family member, Bcl-xL, also shows significant overexpression in some types of lung and ovarian cancers. Although the precise mechanism of Bcl-2 family mediated apoptosis is the subject of considerable debate,³ it is generally agreed that apoptosis is inhibited by the binding of the pro-death proteins to their anti-apoptotic counterparts. Bcl-2 (and Bcl-xL) have a binding groove that accommodates the BH3 (Bcl-2 Homology-3) domain of pro-apoptotic family members,⁴ preventing their oligomerization and the initiation of the apoptosis cascade.⁵ Chimaeric Bcl-2/xL NMR and X-ray crystal structures have demonstrated that the binding groove is amenable to small molecule intervention and studies have shown that such molecules are able to sensitise tumour cells to apoptosis.⁶ Such molecules should abrogate the anti-apoptotic effects of Bcl-2 expression and chemosensitize a significant proportion of tumours to cell death by existing cytotoxics and new targeted therapies.

This has been most successfully demonstrated with ABT-263, a small molecule Bcl-2/Bcl-xL inhibitor that has entered clinic trials.⁷



We have described the discovery and SAR of a series of 1,2,3,4-tetrahydroisoquinoline (THIQ) amide substituted phenyl pyrazoles, such as **1** and **2**, that display good selectivity and potency against Bcl-2.⁸ These molecules often exhibited appreciable line broadening in their ¹H NMR spectra due to the restricted rotation around the Ar-(C=O)-N bond. Substitution at the THIQ 3-position led to the observation of individual rotamers by NMR. Although atropisomeric⁹ molecules have been identified through drug discovery programmes,¹⁰ the presence of multiple conformational forms adds to the complexity of the development

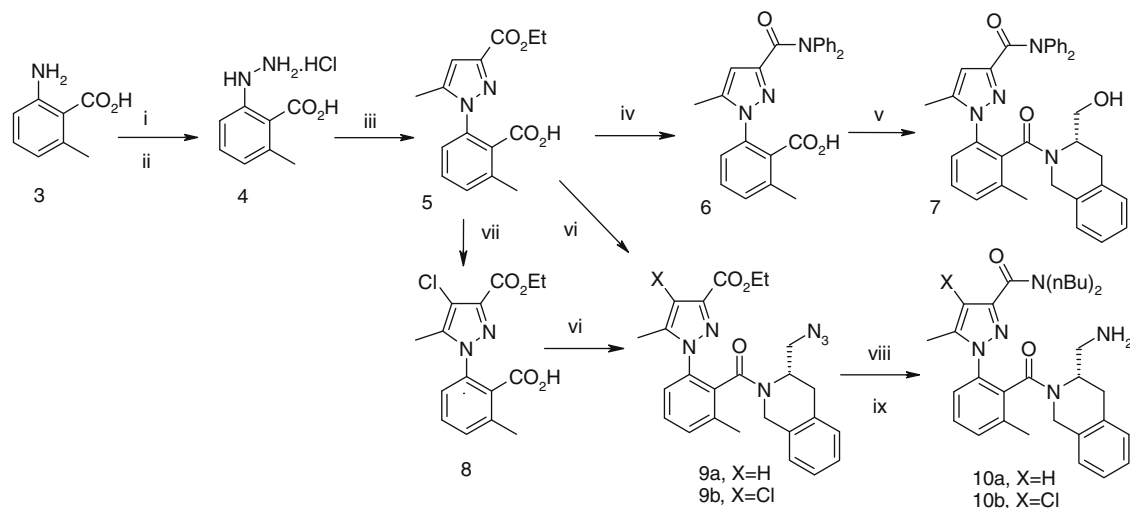
* Corresponding author. Tel.: +44 1753 534655.

E-mail address: john.porter@ucb-group.com (J. Porter).

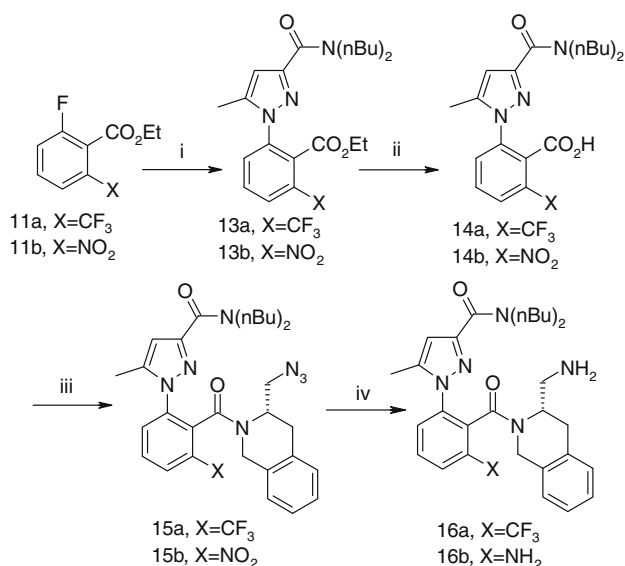
process, consequently, there have been a number of reports of attempts to overcome these issues.¹¹ However, we postulated that by sufficiently restricting rotation by substitution at the phenyl 6-position, it would be possible to physically separate and characterise the individual rotameric species. Assuming that Bcl-2 recognises only one ligand conformation, then the protein would select the bioactive conformation on exposure to the rotameric mixture. We could then determine the conformation by ¹H NMR techniques and optimise the molecule by a process of structure based drug design. The results of this work are described in this paper.

The phenylpyrazoles were prepared according to the method outlined in Scheme 1. The benzoic acid **3** was converted to the hydrazine **4** and cyclised with ethyl acetoxypruvate to give the pyrazole **5**. Conversion to the amide **6** was achieved with lithiated diphenylamine followed by coupling with the THIQ to give **7**. Alternatively, the azide substituted THIQ was coupled to the acid chloride derived from **5** followed by hydrogenolysis to give the amine **10a**. Introduction of a chlorine atom at the pyrazole 4-position was achieved by treating acid **5** with *N*-chlorosuccinimide, followed by a similar sequence of reactions yielding amine **10b**. The route depicted in Scheme 2 allowed greater flexibility in the incorporation of the group ortho to the phenyl carboxylate. Base induced coupling of the pyrazole **12** (prepared by the reaction of the dibutyl amino aluminate with the pyrazole ethyl ester) with the fluoride **11** was followed by hydrolysis of the ester and pyB-ROP mediated coupling with the azide substituted THIQ to give **15** which was reduced to give the final product **16**.

Slow rotation around the Ar-THIQ amide bonds give four atropisomers, two orientations for the amide (*s-cis* and *s-trans*) and two for the aryl carbonyl (axial-*R* and axial-*S*) (Fig. 1). These were evident in the ¹H NMR spectrum of **1** where the 4-pyrazole proton signals proved to be diagnostic, displaying four resonances between δ 5.5 and δ 6.1 (in CD₃OD, 25 °C) with an integral ratio of 1:2:2:8 (corresponding to the four rotamers shown in Fig. 1, R = H), although only one peak was observed by HPLC. One other feature of the ¹H NMR spectrum were the signals associated with the THIQ C-1 methylene diastereotopic protons which appeared as doublets but with very large chemical shift differences between the signals corresponding to the α and β protons and the C-3 methine proton. The magnitude of this effect, caused by shielding/deshielding by the amide carbonyl, was dependent on whether the protons were



Scheme 1. Reagents and conditions: (i) NaNO₂, aq HCl, 0 °C, 30 min; (ii) SnCl₂, HCl, 25 °C, 3 h; (iii) ethyl acetoxypruvate, gAcOH, reflux, 1 h; (iv) Ph₂NH, *n*BuLi, THF, -78 to 25 °C; (v) (S)-1-(1,2,3,4-tetrahydro-isoquinolin-3-yl)-methanol, HOAT, EDCI, NMM, CH₂Cl₂, 25 °C, 16 h; (vi) (S)-3-azidomethyl-1,2,3,4-tetrahydro-isoquinoline, (COCl)₂, CH₂Cl₂, 25 °C, 16 h; (vii) NCS, CCl₄, 25 °C, 16 h; (viii) *n*Bu₂NH, EDCI, HOBT, Et₃N, 25 °C, 16 h; (ix) 10% Pd-C, H₂, EtOH, 25 °C, 1 h.



Scheme 2. Reagents and conditions: (i) 5-methyl-1*H*-pyrazole-3-carboxylic acid dibutylamide **12**, Cs₂CO₃, DMF, 110 °C, 2 h; (ii) LiOH, THF, water, 25 °C, 16 h; (iii) (S)-3-azidomethyl-1,2,3,4-tetrahydro-isoquinoline, pyBROP, DIEA, CH₂Cl₂, 18 °C, 16 h; (iv) 10% Pd-C, H₂, EtOAc, 25 °C, 24 h.

cis or *trans* to the carbonyl. This analysis allowed the conformation of the THIQ moiety system to be determined with the 3-substituent in a theoretically energetically less favoured pseudo-axial position. This is a manifestation of a special case of the A-1,3 strain which is commonly observed in substituted acylated cyclic amines.¹² The methyl substituted analogue, **7**, (Fig. 1, R = Me) also showed four pyrazole proton signals (Fig. 4) but this time the ratio changed on equilibration (DMSO, 25 °C) from 1:6.4:1:2.4 at *t* = 0 h to 1:1.5:0.2:1.3 at *t* = 48 h.

The atropisomers of **7** were sufficiently stable to enable HPLC separation¹³ and isolation, the ¹H NMR of the separated components is shown in Figure 4. The separated rotamers were screened in the Bcl-2 assay (Table 1).¹⁴ Fraction 2 is clearly the most active, however, the other three fractions retained some activity, particularly fraction 4. This was believed to be due to re-equilibration of the separated rotamers during the

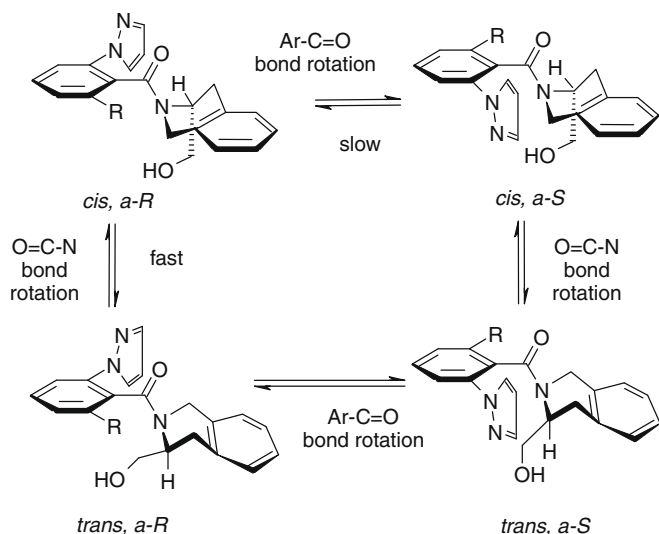


Figure 1. Inter-conversions between the four isomers of compound **7**: *cis* and *trans* are used to denote the relative configuration between the carbonyl oxygen and the 3-THIQ substituent in the amide moiety; *R* and *S* denote the axial chirality arising from the restricted rotation around the Ar-C=O bond. The pyrazole substituent has been simplified in the interests of clarity.

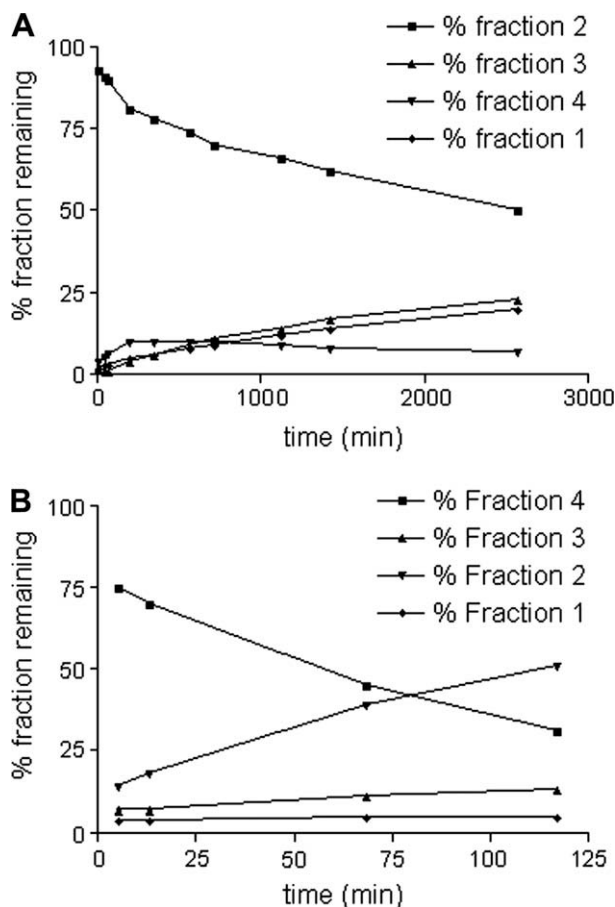


Figure 2. (A) Re-equilibration of compound **7** fraction 2 in DMSO solution at RT, as determined by integration of the pyrazole 4-H ^1H NMR signal. (B) Re-equilibration of compound **7** fraction 4 in DMSO solution at RT, as determined by integration of the pyrazole 4-H ^1H NMR signal.

time of the experiment. To further investigate this, the re-equilibration of the isolated rotamers in DMSO solution was followed

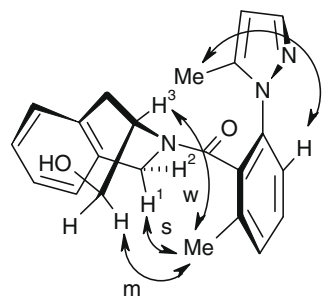


Figure 3. The *cis*, *a-R* (bioactive) atropisomer of compound **7** showing observed nOe interactions (s = strong, m = medium, w = weak). The diastereotopic protons on the THIQ C-1 and C-3 atoms are labelled. The pyrazole ring has been simplified for clarity.

experimentally by monitoring the change in integrated signal area of the pyrazole 4-H ^1H NMR signals with time, the examples for fractions 2 and 4 are shown in Figure 2. The curves show that the rate of equilibration of fraction 2 (Fig. 2A) is relatively slow with approximately 90% of fraction 2 remaining after 90 min (the approximate time course of the LANCE assay). However, inter-conversion from fraction 4 to fraction 2 is fast (Fig. 2B) with approximately 40% of fraction 2 present after 90 min. The apparent activity of fraction 4 may therefore be explained as a result of the rapid conversion to the active rotamer, fraction 2. Attempts to measure the energy of the barrier to rotation by observation of the coalescence of the NMR signals of the diastereotopic protons with increasing temperature were unsuccessful because of the high temperatures required (no coalescence of peaks in the 600 MHz ^1H spectrum of the equilibrium mixture in DMSO- d_6 was observed at 50 °C). The barrier to rotation around the amide bond of 2,6-disubstituted aryl amides has been reported to be in excess of 100 kJ mol $^{-1}$.¹⁵ No attempt at lineshape analysis has been made at this time.

The 1D selective pulse ^1H NMR nOe spectra of the four separated atropisomers were measured and, as expected, found to give a unique pattern of cross-peaks indicative of their conformational differences, an example of the nOe interactions is shown in Figure 3. A simple molecular mechanics model of **7** was generated using Sybyl¹⁶ and low energy conformations determined for each of the four rotameric forms. It then proved possible to uniquely assign the nOe information for each of the physically isolated rotameric forms to the appropriate geometry of the models, and thus assign the rotameric conformations of the models to the physically separated compounds. As the activity against Bcl-2 of the separated atropisomers was known, it was possible to assign the conformation of the active rotamer as *cis*, *a-R* (Table 1). From the assignment of the above conformers, it was possible to predict the equilibria between each peak through single, stepwise bond rotations, summarised in Figure 1. These equilibria correlate with those observed experimentally in the ^1H NMR time-course equilibrations described above.

A Bcl-2 affinity assay gave further evidence for the identity of the atropisomeric eutomer of **7**.¹⁷ Bcl-2 protein was added to the equilibrium mixture of rotamers, resulting in only the active conformer binding to Bcl-2. The compound/protein complex was separated from unbound compound by size exclusion chromatography, the complex denatured with acetonitrile to release the compound which was isolated and characterised by LC-MS (Fig. 3). The results are in agreement with the Bcl-2 assay findings: the rotamer corresponding to HPLC fraction 2 was the major component of the isolated fraction (Fig. 5). (The presence of other rotamers observed is due to flow-through.)

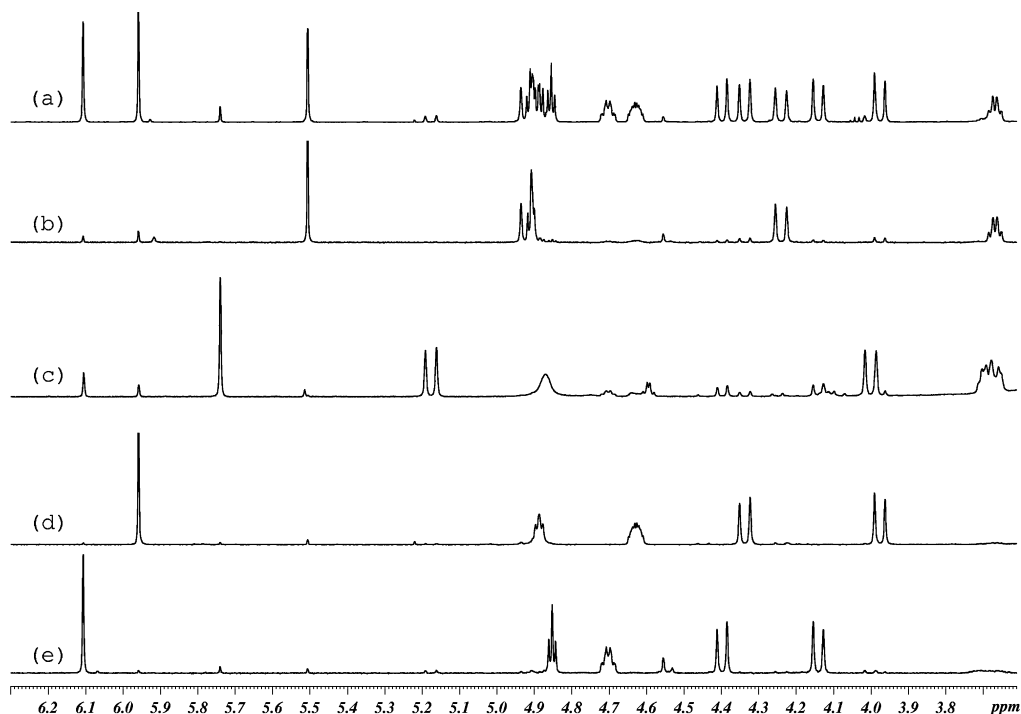


Figure 4. The ^1H NMR spectra (600 MHz) of **7** showing the diagnostic region between δ 3.6 and δ 6.3. (a) The equilibrium mixture after 48 h, (b) fraction 1, (c) fraction 4, (d) fraction 3, (e) fraction 2.

Table 1
Bcl-2 activity, 600 MHz NMR data and assignment of the atropisomeric forms of compound **7**

Compound	HPLC	Assignment	Pyrazole 4-H δ	H ¹ , H ² δ	H ¹ , H ² J (Hz)	H ³ δ	Bcl-2 IC ₅₀ (nM)
7	Mixture	–	–	–	–	–	600
7	Fraction 1	<i>trans</i> , a-S	5.51	4.92, 4.24	18.0	3.67	1100
7	Fraction 2	<i>cis</i> , a-R	6.11	4.40, 4.14	16.0	4.70	210
7	Fraction 3	<i>cis</i> , a-S	5.96	4.33, 3.98	16.8	4.63	6100
7	Fraction 4	<i>trans</i> , a-R	5.74	5.18, 4.00	17.8	3.68	390

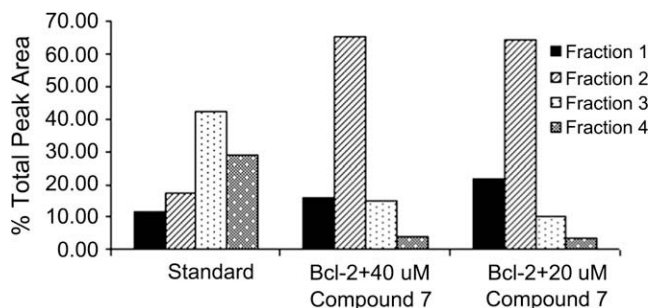


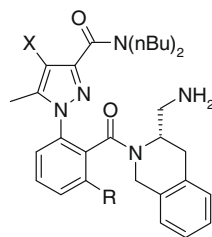
Figure 5. Plot of the HPLC peak area for the 4 rotamers of **7** following incubation with Bcl-2, size exclusion chromatography to remove unbound ligand and protein denaturation to release the bioactive conformation. The plot should be compared with the standard equilibrium mixture shown on the left to see the clear enrichment of fraction 2.

A limited SAR study was conducted on analogues of **7** (Table 2). Replacement of the pyrazole diphenyl amide with dibutyl groups has been shown to give improved potency against Bcl-2.⁸ Compound **10a**, which, at equilibrium, exists as two major conformers was separated and analysed by NMR in a similar fashion to that described above to show that the bioactive conformer, fraction 1, had

the equivalent conformation at the THIQ amide as compound **7**. The apparent activity of fraction 2 is due to the presence of approximately 20% of fraction 1 as an impurity. The chloro analogue, **10b** was not separated but the equilibrium mixture was even more potent than **10a**. We surmise that the chloro group locks the di-*n*-butylamide in a favourable position. The equilibrium mixture of **16a** exists as two major conformers and was readily separable, but both conformers were inactive. The amino analogue **16b** was also less active, the conformation of these species was not determined. Following the conclusion of this work, an X-ray crystal structure of a close analogue, **1** complexed with a soluble mutant of the Bcl-2 protein was solved.^{8,18} This structure confirmed that the bound conformation had the same rotameric conformation as the active fraction (fraction 2) of **7** (see Fig. 6). This work and our SAR observations⁸ shows that the conformation of the THIQ group plays a significant role in determining the potency of these molecules.

Armed with this information we set about designing molecules that would be locked into the bioactive conformation to afford enhanced potency and remove the issues associated with the development of atropisomeric drugs. In conclusion, we have utilised the atropisomeric properties of some potent inhibitors of Bcl-2 to identify the bioactive conformation of these compounds.

Table 2
Bcl-2 activity and 600 MHz NMR data for the atropisomeric forms of analogues of compound 7



Compound	R	X	HPLC	Pyrazole 4-H δ	H ¹ , H ² δ	H ¹ , H ² J (Hz)	H ³ δ	Bcl-2 IC ₅₀ (nM)
10a	Me	H	Mixture	–	–	–	–	175
			Fraction 1	6.33	4.44, 4.29	16.6	4.61	55
			Fraction 2	6.46	4.27, 4.15	16.6	4.54	358
			Fraction 3	6.36	4.84, 4.19	18.0	3.76	nd
			Fraction 4	6.43	5.21, 3.85	18.0	3.69	nd
10b	Me	Cl	Mixture	n/a	–	–	–	42
			Fraction 1	6.35	4.35, 4.18	16.2	4.50	16% at 30 μ M
16a	CF ₃	H	Fraction 1	6.35	4.35, 4.18	16.2	4.50	16% at 30 μ M
			Fraction 2	6.43	4.24, 4.07	16.7	4.46	14,400
16b	NH ₂	H	Mixture	–	–	–	–	1070

Compound **10a** fractions 3 and 4 were not physically separated, their NMR data was determined from the spectrum of the mixture, nd = not done.

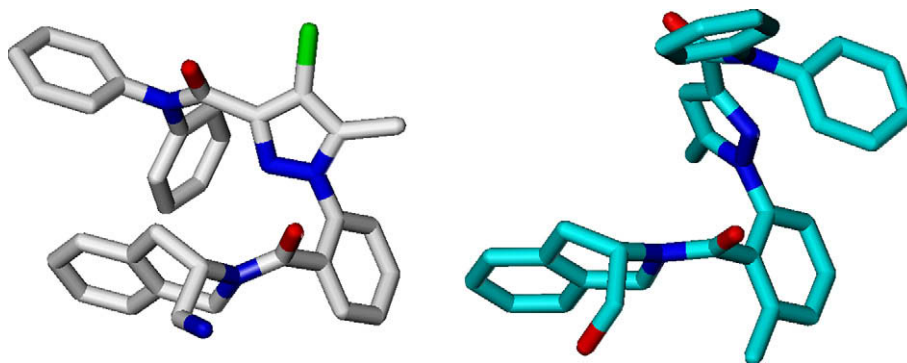


Figure 6. The X-ray conformation of **1** (white) and the nOe-derived solution-phase conformation model of the *cis*, *a*-R bioactive atropisomer of **7** (cyan). Comparison of the structures shows that they share a common rotameric conformation about the THIQ amide. The absence of nOe information relating to the diphenyl amide prevents assignment of a preferred orientation of this group, however it is likely that this part of the molecule rotates freely in solution.

References and notes

- (a) Youle, R. J.; Strasser, A. *Nat. Rev. Mol. Cell Biol.* **2008**, *9*, 47; (b) Cory, S.; Adams, J. M. *Nat. Rev. Cancer* **2002**, *2*, 647.
- Berghella, A. M.; Pellegrini, P.; Contasta, I.; Del Beato, T.; Adomo, D. *Cancer Biother. Radiopharm.* **1998**, *13*, 225.
- Chipuk, J. E.; Green, D. R. *Trends Cell Biol.* **2008**, *18*, 157.
- (a) Peteros, A. M.; Medek, A.; Nettlesheim, D. G.; Kim, D. H.; Yoon, H. S.; Swift, K.; Matayoshi, E. D.; Oltersdorf, T.; Fesik, S. W. *Proc. Nat. Acad. Sci. U.S.A.* **2001**, *98*, 3012; (b) Muchmore, S. W.; Sattler, M.; Liang, H.; Meadows, R. P.; Harlan, J. E.; Yoon, H. S.; Nettlesheim, D.; Chang, B. S.; Thompson, C. B.; Wong, S.-L.; Ng, S.-C.; Fesik, S. W. *Nature* **1996**, *381*, 335; (c) Sattler, M.; Liang, H.; Nettlesheim, D.; Meadows, R. P.; Harlan, J. E.; Eberstadt, M.; Yoon, H. S.; Chang, B. S.; Minn, A. J.; Thompson, C. B.; Fesik, S. W. *Science* **1997**, *275*, 983; (d) Petros, A. M.; Nettlesheim, D. G.; Wang, Y.; Olenjniczak, E. T.; Meadows, R. P.; Mack, J.; Swift, K.; Matayoshi, E. D.; Zhang, H.; Thompson, C. B.; Fesik, S. W. *Protein Sci.* **2000**, *9*, 2528.
- Huang, Z. *Chem. Biol.* **2002**, *9*, 1059.
- (a) Oltersdorf, T.; Elmore, S. W.; Shoemaker, A. R.; Armstrong, R. C.; Augeri, D. J.; Belli, B. A.; Bruncko, M.; Deckwerth, T. L.; Dinges, J.; Hajduk, P. J.; Joseph, M. K.; Kitada, S.; Korsmeyer, S. J.; Kunzer, A. R.; Letai, A.; Li, C.; Mitten, M. J.; Nettlesheim, D. G.; Ng, S.-C.; Nimmer, P. M.; O'Connor, J. M.; Oleksijew, A.; Petros, A. M.; Reed, J. C.; Shen, W.; Tahir, S. K.; Thompson, C. B.; Tomaselli, K. J.; Wang, B.; Wendt, M. D.; Zhang, H.; Fesik, S. W.; Rosenberg, S. H. *Nature* **2005**, *435*, 677; (b) Lee, E. F.; Czabotar, P. E.; Smith, B. J.; Deshayes, K.; Zobel, K.; Colman, P. M.; Fairlie, W. D. *Cell Death Differ.* **2007**, *14*, 1711.
- (a) Tse, C.; Shoemaker, A. R.; Adickes, J.; Anderson, M. G.; Chen, J.; Jin, S.; Johnson, E. F.; Marsh, K. C.; Mitten, M. J.; Nimmer, P.; Roberts, L.; Tahir, S. K.; Xiao, Y.; Yang, X.; Zhang, H.; Fesik, S.; Rosenberg, S. H.; Elmore, S. W. *Cancer Res.* **2008**, *68*, 3421; (b) Park, C.-M.; Bruncko, M.; Adickes, J.; Bauch, J.; Ding, H.; Kunzer, A.; Marsh, K. C.; Nimmer, P.; Shoemaker, A. R.; Song, X.; Tahir, S. K.; Tse, C.; Wang, X.; Wendt, M. D.; Yang, X.; Zhang, H.; Fesik, S. W.; Rosenberg, S. H.; Elmore, S. W. *J. Med. Chem.* **2008**, *51*, 6902.
- (a) Porter, J.; Payne, A.; de Candole, B.; Ford, D.; Hutchinson, B.; Trevitt, G.; Turner, J.; Edwards, C.; Watkins, C.; Whitcombe, I.; Davis, J.; Stubberfield, C. *Bioorg. Med. Chem. Lett.* **2009**, *19*, 230; b) Payne, A.; Porter, J.; Watkins, C.; Edwards, C.; Ford, D.; de Candole, B.; Hutchinson, B.; Turner, J.; Lemmens, I.; Tavernier, J.; Davis, J.; Stubberfield, C.; *Abstracts of Papers, Molecular Targets and Cancer Therapeutics EORTC-AACR-NCL*, San Francisco CA, USA, October 22–26, 2007; B297.
- Oki, M. *Top. Stereochem.* **1983**, *14*, 1.
- For example, see: (a) Guile, S. D.; Bantick, J. R.; Cooper, M. E.; Donald, D. K.; Eyssade, C.; Ingall, A. H.; Lewis, R. J.; Martin, B. P.; Mohammed, R. T.; Potter, T. J.; Reynolds, R. H.; St-Gallay, S. A.; Wright, A. D. *J. Med. Chem.* **2007**, *50*, 254; (b) Vrudhula, V. M.; Dasgupta, B.; Qian-Cutrone, J.; Kozlowski, E. S.; Boissard, C. G.; Dworetzky, S. I.; Wu, D.; Gao, Q.; Kimura, R.; Gribkoff, V. K.; Starrett, J. E., Jr. *J. Med. Chem.* **2007**, *50*, 1050; (c) Palani, A.; Shapiro, S.; Clader, J. W.; Greenlee, W. J.; Blythin, D.; Cox, K.; Wagner, N. E.; Strizki, J.; Baroudy, B. M.; Dan, N. *Bioorg. Med. Chem. Lett.* **2003**, *13*, 705, and references therein.
- (a) Ishichi, Y.; Ikeura, Y.; Natsugari, H. *Tetrahedron* **2004**, *60*, 4481; (b) Albert, J. S.; Ohnmacht, C.; Bernstein, P. R.; Rumsey, W. L.; Aharony, D.; Alelyunas, Y.; Russell, D. J.; Potts, W.; Sherwood, S. A.; Shen, L.; Dedinas, R. F.; Palmer, W. E.; Russell, K. J. *Med. Chem.* **2004**, *47*, 519.
- Malhotra, S. K.; Johnson, F. *Chem. Commun.* **1968**, *19*, 1149.
- HPLC separation of compound **7** was performed using a Waters HPLC system controlled by Fractionlynx software fitted with a Phenomenex Gemini 10 μ m C18 110 Å 150 × 21 mm HPLC column (Phenomenex, Macclesfield, Cheshire, UK). Mobile phase composition of 0.1% formic acid in water + 10% acetonitrile (phase A) and 0.1% formic acid in acetonitrile + 10% water (phase B). 0–0.5 min, 95% A 5% B; 0.5–9.5 min, 50% A 50% B; 9.5–10 min, 40% A 60% B; 10–11.5 min, 5% A 95% B; 11.5–12 min, 95% A 5% B, at a constant flow rate of 20 mL/min. The compound was dissolved in DMSO (10 mg/mL, 250 μ L) and loaded onto the

column through a 500 μ L injection loop. Fractions were collected automatically into test tubes that were combined as necessary. Solvent was immediately removed by rotary evaporation followed by freeze drying.

14. HTRF-LANCE assays detected interactions of Bcl-2 proteins expressed as GST-fusion proteins and biotinylated 16-mer BH3 peptides. Interactions were detected using europium-conjugated anti-GST antibody and APC-labelled streptavidin (Perkin-Elmer) using a Wallac Victor 2 plate reader.
15. Ahmed, A.; Bragg, A.; Clayden, J.; Lai, L. W.; McCarthy, C.; Pink, J. H.; Westlund, N.; Yasin, S. A. *Tetrahedron* **1998**, *54*, 13277.
16. Tripos Software, Inc., St. Louis, MO, USA.
17. Recombinant Bcl-2 protein was diluted to 40 μ M in Assay Buffer (25 mM Tris-Cl, pH 7.4, 150 mM NaCl, 0.1% β -lactoglobulin). An equal volume of compound was added in 2% DMSO in Assay Buffer and the mixture incubated for 5 min at 4 $^{\circ}$ C. Protein-compound complexes were separated from unbound compound by passing through a Protein Desalting Spin Column. Complexes were denatured in an equal volume of acetonitrile and characterised by LC-MS.
18. PDB code 2W3L.